Research Article

In Silico and *In Vitro* Antiviral Activity Evaluation of Prodigiosin from *Serratia marcescens* Against Enterovirus 71

Muhamad Fakrulnizam Abd Aziz, Chee Wai Yip and Norefrina Shafinaz Md Nor*

Department of Biological Sciences and Biotechnology, Faculty of Science and Technology, Universiti Kebangsaan Malaysia,
43600 Bangi, Selangor
*Corresponding author: efrina@ukm.edu.my

ABSTRACT

Prodigiosin, a red linear tripyrrole pigment found in *Serratia marcescens*, is one such naturally occurring compound that has gained wide attention owing to its numerous biological activities, including antibacterial, antifungal, antimalarial, anticancer, and immunosuppressive properties. This study was conducted to evaluate the possible antiviral activity of prodigiosin against Enterovirus 71, a causative agent of hand, foot, and mouth disease (HFMD). Preliminary studies were done *in silico* by analyzing the interaction of prodigiosin with amino acid residues of five EV71-target proteins. Interaction refinement analysis with FireDock revealed that 2C helicase (-48.01 kcal/moL) has the most negative global energy, followed by capsid (-36.52 kcal/moL), 3C protease (-34.16 kcal/moL), 3D RNA polymerase (-30.93 kcal/moL) and 2A protease (-20.61 kcal/moL). These values are indicative of the interaction strength. Prodigiosin was shown to form chemical bonds with specific amino acid residues in capsid (Gln-30, Asn-223), 2A protease (Trp-33, Trp-142), 2C helicase (Tyr-150, His-151, Gln-169, Ser-212), 3C protease (Glu-50), and 3D RNA polymerase (Ala-239, Tyr-237). To investigate further, prodigiosin was extracted from *S. marcescens* using a methanolic extraction method. *In vitro* studies revealed that prodigiosin, with an IC_{50} value of 0.5112 μg/mL, reduced virus titers by 0.17 log (32.39%) in 30 min and 0.19 log (35.43%) in 60 min. The findings suggest that prodigiosin has antiviral activity with an intermediate inhibitory effect against EV71. As a result of this research, new biological activities of prodigiosin have been identified.

Key words: Cytotoxicity, FireDock, HFMD, MTT, prodigiosin, virucidal

INTRODUCTION

According to the World Health Organization (2018), numerous cases of hand, foot, and mouth disease (HFMD) have been reported in countries throughout the Western Pacific region, including Malaysia, Japan, the Republic of Korea, Singapore, Vietnam, and China. As of June 2022, the Malaysian Ministry of Health (MoH) has reported over 95,000 HFMD cases, which is over the warning threshold (1,215 cases) indicated by the ministry (Abdullah, 2022). HFMD is a complex of the febrile disease characterized by cutaneous eruptions (exanthem) on the palm of the hands and feet with simultaneous occurrences of muco-cutaneous vesiculo-ulcerative lesions in the mouth (Chua & Kasri, 2011). HFMD has been an important public health concern due to its high propensity to cause large outbreaks and even deaths among children and infants (Fong *et al*., 2021).

HFMD is a systemic infection caused by human enteroviruses and is frequently associated with Coxsackievirus A16 (CA16) and Enterovirus 71 (EV71) as its etiological agents, which are non-enveloped RNA viruses (Ren *et al*., 2015; Yuan *et al*., 2018). Most patients suffering from HFMD manifest mild clinical courses and are self-limiting meaning that the disease disappears on its own or does not have long-term adverse effects on health. However, several reported cases, especially those caused by EV71, tend to be more severe in symptoms and can lead to death (Kim

et al., 2018). EV71 is the second most important neurotrophic enterovirus after poliovirus and infections of EV71 can lead to severe neurologic, cardiac, and respiratory complications in children below the age of 5. Apart from that, EV71 has been associated with various other clinical diseases such as meningitis, encephalitis, and poliomyelitis-like acute paralysis (Chua & Kasri, 2011). HFMD can be easily transmitted via droplet transmission and fomite amongst children in care centers and kindergartens (Sun *et al*., 2018). As a result, it is a significant disease in terms of public health.

Treatment for HFMD is primarily supportive (treating symptoms) due to the absence of specific antiviral agents against its causative agent. Patients will usually recover from the disease within 7 to 10 days. Patients are closely monitored from time to time to ensure they are well hydrated, while other symptoms like fever and pain are controlled with non-steroidal anti-inflammatory drugs (NSAIDs) and acetaminophen. Additionally, the liquid mixture of ibuprofen and diphenhydramine can be used as a gargling solution to relieve pain resulting from ulcers (Coates *et al*., 2019; Rasti *et al*., 2019).

Currently, there are no drugs against the causative agent of HFMD that have been approved. Several EV71 vaccine candidates are being developed (in the clinical trial stage), using viral structural proteins as immunogens to produce antibodies, which target viral epitope neutralization (Fang & Liu, 2018; Li *et al*., 2021). These include inactivated viruses, live-attenuated viruses, and viral-like particle vaccines. There is no proven pharmacological method to prevent or control HFMD/EV71 and the main action frequently taken involves a non-pharmaceutical approach in which most of the parts are aimed at interfering with the viral transmission chain (CDC, 2022). Early detection, identification, and intervention of the outbreak in high-risk cases from potentially developing into a more severe condition is the main key to minimizing the impact of the disease. Hence, there is always a constant need for antiviral agent discovery and development efforts to combat the recurrent endemic of HFMD that poses a threat to global public health.

The red pigment of prodigiosin is synthesized under both aerobic and anaerobic conditions by the facultative anaerobe bacterium called *Serratia marcescens* from the family of Enterobacteriaceae (Wei & Chen, 2005). Physiologically, the role of prodigiosin in the producing bacterial strain is unknown, yet numerous biological activities related to prodigiosin have been reported previously. These include antifungal, antiproliferative, and immunosuppressive activities (De Araújo *et al*., 2010). Moreover, Lapenda *et al*. (2015) reported bactericidal and bacteriostatic effects of prodigiosin, whereas Lin *et al*. (2019) demonstrated prodigiosin

to possess high apoptotic activity on cancer cell lines and low cytotoxicity on non-cancer cells. Unlike vaccines, most natural products (such as prodigiosin) and antiviral drugs, use both viral structural and non-structural proteins as targets for direct inactivation upon their binding to the active sites, rendering the viral proteins inactive or incapable of functioning properly (Su *et al*., 2020; Littler *et al*., 2021). On the other hand, *in silico* studies and molecular docking analysis on prodigiosin with several RNA virus target proteins such as HBV, HIV, and H1N1 suggested the presence of antiviral activity from prodigiosin when interactions with the aforementioned viral protein active sites are found (Suba *et al*., 2013).

Although prodigiosin has been reported to possess antimicrobial activities against various microbes, no experimental data is proving the antiviral activity of prodigiosin against human viruses. The *in silico* studies of prodigiosin conducted in previous research were putative antiviral potential against enveloped human viruses but the antiviral efficacy against non-enveloped human viruses is yet to be determined. Hence, in this study, we aim to predict the potential interaction between prodigiosin and essential viral proteins of EV71 through *in silico* analysis and evaluate its antiviral efficacy through *in vitro* antiviral assay.

MATERIALS AND METHODS

Molecular docking

Protein structures used in this research were downloaded from the Protein Data Bank (PDB) (http://rcsb.org). EV71 target protein candidates were chosen (based on their critical role in the virus) as receivers, and they were expected to interact positively with the prodigiosin pigment compound. The prodigiosin structure (PubChem CID: 135408511), as a ligand, with a molecular formula of $C_{20}H_{25}N_3O$, was chosen from PubChem (https://pubchem.ncbi.nlm.nih.gov/compound/Prodigiosin). The prodigiosin 3D chemical structure file downloaded from PubChem was converted from SDF file format (*input*) to PDB file format (*output*) using an online SMILES translator and structure file generator (https://cactus.nci.nih.gov/translate/), which is a public web server of the Computer-Aided Drug Design (CADD) Group.

Protein-ligand docking was conducted using the DockThor web server (https://dockthor.lncc.br/v2/) and the output of the binding affinity value was generated. The geometrical orientation, conformational complementarity, and the characteristics between the protein and the ligand were evaluated. The interaction results were analyzed based on the binding affinity value (kcal/moL) of prodigiosin (ligand) to EV71 target proteins. Additionally, PatchDock (http://bioinfo3d.

cs.tau.ac.il/PatchDock/), a web server with an algorithm based on shape complementarity principles (Schneidman-Duhovny *et al*., 2005) was used. PatchDock generated output such as the geometric score, the interface area size, the desolvation energy, and the actual rigid transformation of the solution.

Subsequently, the fast interaction refinement process in molecular docking was carried out using the FireDock web server (http://bioinfo3d. cs.tau.ac.il/FireDock/), where candidate solutions were further refined and re-scored (Andrusier *et al*., 2007). FireDock generated the lowest global energy value as the output of all of the candidates for protein-ligand complexes. Visualization of the protein-ligand complexes was done using PyMOL (version 2.3.5), a molecular visualization system software. Also, PyMOL was used to visualize amino acid residues on the virus target protein active site chains that form chemical bonds with prodigiosin, including the nucleus-to-nucleus distance (in angstrom, Å).

Bacterial culture
Serratia marcescens UKMCC 1014 was procured from the Universiti Kebangsaan Malaysia Culture Collection (UKMCC), Bangi, Malaysia. *S. marcescens* UKMCC 1014 was grown on peptone glycerol agar at 28 °C for 96 h. For the prodigiosin pigment production, *S. marcescens* UKMCC 1014 was inoculated into a sterile cold peptone glycerol broth medium followed by incubation in an orbital shaker incubator at 28 °C for 96 h.

Methanolic extraction of prodigiosin
The prodigiosin from *S. marcescens* UKMCC 1014 was extracted using a methanolic extraction method as described by Nakashima *et al*. (2005). *S. marcescens* UKMCC 1014 was cultured in 100 mL of yeast extract-peptone-glucose (YPG) broth medium at 28 °C for 96 h. Then, 100 mL of methanol was added to the YPG broth, followed by centrifugation of the mixture at 10,000 × *g* for 30 min. The supernatant was evaporated under a vacuum to obtain the dry residue, which was later extracted into chloroform and washed several times using the same solvent. The extracted fraction was centrifuged at 10,000 × *g* for 10 min. The supernatant was evaporated under a vacuum before the addition of methanol to the dry residue. The dry residue was dissolved thoroughly in methanol. The absorption spectrum of the red pigment was measured using a spectrophotometer with a wavelength ranging from 200 nm to 800 nm (ultraviolet to visible light region).

Cytotoxicity assay
This assay aimed to evaluate the non-cytotoxic concentration that could be used in an antiviral

study. The Vero cells were grown in the Dulbecco's Modified Eagle's Medium (DMEM) containing 5% (v/v) Fetal Bovine Serum (FBS), 100 IU/mL penicillin-streptomycin, 1% (v/v) L-glutamine, 50 μg/mL amphosphate B and sodium bicarbonate ($NaHCO_3$). Cell cultures were incubated and maintained at 37 °C in 5% CO_2 atmospheric conditions. Subsequently, 100 μL of cell suspension was aliquoted into each well in a 96-well microtiter plate and incubated for monolayer cell formation. DMEM was discarded from each well using a micropipette followed by the addition of 200 μL extract, fresh DMEM, or dimethyl sulfoxide (DMSO) and further incubated for 24 h at 37 °C in 5% CO_2 atmospheric condition. Cell concentration (cell/mL) was calculated. Serial dilution of the original extract concentration (100%) was done for extract preparation.

Cell culture was stained for analysis to obtain the IC_{50} value. After incubation, DMEM was discarded and each well was washed using DMEM without 5% FBS a few times. 100 μL DMEM with 5% FBS and 40 μL MTT (concentration: 5 mg/mL) were added to each well. The microtiter plate was fully covered with aluminum foil and incubated for 3 h at 37 °C in 5% CO_2 atmospheric condition. MTT was removed and DMSO was added, converting yellow tetrazole into purple formazan crystal in viable cells. A microtiter plate reader (EpochTM Microplate Spectrophotometer Gen5) was used to measure absorbance at a 570 nm wavelength. The percentage of cell viability was calculated using the following formula:

$$\text{Percentage of cell viability } (\%) = \frac{\text{Test OD-Negative control OD}}{\text{Positive control OD-Negative control OD}} \times 100\%$$

The data from the percentage of cell viability at different extract concentrations was plotted as a graph of cell viability percentage against the log concentration of prodigiosin extract. The IC_{50} value was calculated using the GraphPad Prism 9 software as the antilog of prodigiosin concentration at 50% population cell death. The regression coefficient (R^2) was recorded to show the data was close to a non-linear fitted regression line (curve fit) and the mathematical model used was suitable for the data. The extract concentration of prodigiosin at IC_{50} was later used for the virucidal test.

Virucidal efficacy suspension test
The virucidal efficacy suspension test was performed to determine the potential of prodigiosin to act as a direct-acting antiviral, which inhibits virus particles directly. The EV71 clinical strain retrieved from Virology Laboratory Stock Collection, Faculty of Science and Technology, Universiti Kebangsaan Malaysia, with an initial virus stock of 1×10^6 pfu/ mL was used and treated with prodigiosin at the

ratio of 1 part virus: 9 parts prodigiosin (1.6 μg/mL). The treatment was done at 37 °C for 30 min and 60 min. The treatment was stopped by carrying out serial dilution on the mixture using DMEM (serum-free) which was cooled on ice to reach the dilution that would allow virus plaque enumeration (10^{-1}, 10^{-3}, 10^{-5}, & 10^{-6}). For this test, 95% ethanol was used as a positive control while serum-free DMEM was used as a negative control. The mixture with different dilutions at 100 μL of inoculum volume was subsequently added to the 24-well plate containing the Vero cell monolayer. Virus adsorption was conducted for 2 h at 37 °C and the plate was tilted every 15 min. The free virus was removed with the addition of 1.5% methylcellulose (MCS) into each well. The plate was incubated for 48 h before the crystal violet (CV) staining to visualize the plaque. The number of plaques formed was calculated and the data was converted to virus titer using the formula:

$$\text{Virus titer} = \text{No. of plaque formed} \times \frac{1}{\text{Dilution factor}} \times \frac{1}{0.1 \text{ mL}}$$

The titer value was then transformed to a $\log_{10}$ scale using the formula:

$$\text{Log reduction} = \log_{10} \frac{A \text{ or Negative control}}{B \text{ or Extract treatment}}$$

Then, the relationship between $\log_{10}$ reduction and reduction percentage was also calculated using the formula:

$$\text{Titer reduction percentage (\%)} = \left(1 - 10^{-\text{Log reduction}}\right) \times 100\%$$

Statistical analysis
The half-maximal inhibition concentration (IC_{50}) of prodigiosin was calculated using GraphPad Prism 9 software. The unequal variance two-tailed paired t-test was used to evaluate the statistical significance. The difference between values is considered significant when $p < 0.05$.

RESULTS AND DISCUSSION
EV71 target protein resolution value (Å)
Some of the target protein structures of the EV71 virus were selected from the Protein Data Bank (http://rcsb.org) based on their functional importance to the infection mechanism of the host cells and the replication of EV71 in the host cells. Among the target proteins selected including capsid proteins [important in viral adhesion to host receptors and viral pathogenesis (Tan *et al*., 2013; Yuan *et al*., 2018; Yuan *et al*., 2016)], 2A protease [important in viral polyprotein maturation, cleavage

of eukaryotic initiation factor 4G (eIF4G) and poly (A)-binding protein (Cai *et al*., 2013; Wang *et al*., 2017)], 2C helicase [important in capsid disassembly and replication complex formation (Xia *et al*., 2015; Guan *et al*., 2017)], 3C protease [important in apoptosis induction, innate immunity inhibition and virus polyprotein processing (Li *et al*., 2019; Wen *et al*., 2020)] and RNA-dependent RNA polymerase 3D [main player in genomic RNA replication and genome-associated viral protein uridylation (Chen *et al*., 2013; Li *et al*., 2019)], and only the target protein with a resolution value of 3 Å and below was selected for analysis (Table 1).

It is important to select target proteins with good resolution values. Resolution is the data quality measure that has been collected on crystals containing proteins or nucleic acids and is defined as the minimum distance of the crystal lattice plane that allows X-ray diffraction to be measured (Wlodawer *et al*., 2008). Proteins in the crystal are aligned and will scatter the X-ray to produce a diffraction pattern that shows the crystal's fine details. Hence, the resolution is the measure of the diffraction details and the details that will be observed when the electron density map is calculated. The majority of protein structures have a resolution of between 1 Å and 3 Å. Structures with the highest order and when the atoms in the electron density map are visible are categorized as high-resolution structures (resolution value of 1 Å or so), whereas structures that show only the basic contours of the protein chain are categorized as low-resolution structures (resolution value of 3 Å & above) (Protein Data Bank, 2022).

Docking analysis
Docking analysis was conducted using different web servers such as DockThor, PatchDock, and FireDock that have been chosen to increase the confidence in the presence of protein-ligand interactions and as a means to compare the data generated from different algorithms employed by each docking platform. The results from the docking of target proteins with prodigiosin (as a ligand) demonstrated the occurrence of protein-ligand interaction for all of the five EV71 target proteins (as a receptor). The docking analysis results generated from these web servers can be summarized in Table 2. The EV71 target proteins with different and multiple localizations to that of the virus, including the viral external proteins such as capsid and viral internal proteins, which have been the major targets of antiviral drugs based on previous reports (Lei *et al*., 2015; Pourianfar & Grollo, 2015; van der Linden *et al*., 2015; Lin *et al*., 2019) were chosen to study the probability of the prodigiosin's suitability for use as a virucidal drug or a post-treatment drug or both.

Table 1. List of EV71 target proteins downloaded from the Protein Data Bank (PDB)

No.	PDB ID	Target protein	Resolution (Å)
1	3VBH	Capsid	2.30
2	3W95	2A Protease	1.85
3	5GQ1	2C Helicase	2.49
4	3OSY	3C Protease	2.99
5	3N6L	3D RNA Polymerase	2.60

Table 2. Analysis of protein-ligand complex interactions in docking

Protein-ligand	Binding Affinity (kcal/moL)	Shape Complementarity Score	Global Energy (kcal/moL)
Capsid-prodigiosin	-7.361	5026	-36.52
2A Protease-prodigiosin	-6.113	4904	-20.61
2C Helicase-prodigiosin	-8.018	5420	-48.01
3C Protease-prodigiosin	-8.162	4792	-34.16
3D RNA Polymerase-prodigiosin	-8.131	4918	-30.93

The binding affinity value of the most negative was given by 3C protease (-8.162 kcal/moL) > 3D RNA polymerase (-8.131 kcal/moL) > 2C helicase (-8.018 kcal/moL) > capsid (-7.361 kcal/moL) > 2A protease (-6.113 kcal/moL). Based on the binding affinity value, prodigiosin has shown the ability to bind tightly and stably on 3C protease, 3D RNA polymerase, 2C helicase, and capsid with a more negative value than -7000 kcal/moL (except for 2A protease). These values were significant because they indicated the potency of a drug. In a study done by Peele *et al*. (2020), several antiviral substances had been tested via computational simulation, and reported that those drugs that fall within an approximate docking score of -7.429 kcal/moL to -10.574 kcal/moL (or even more negative) were as potent if tested *in vivo*. From this finding, it was predicted the activity of prodigiosin was likely to target two different mechanisms, namely in virucidal activity and post-treatment. Nevertheless, prodigiosin binding affinity was higher post-treatment. Also, the lack of EV71 external protein diversity as targets was one of the contributing factors because only one external protein was used in the screening (for virucidal effect).

To address the issue, additional analysis was performed using various docking platforms to increase confidence, thereby validating the findings of the mechanism. Comparative analysis of a few docking algorithms was deemed to increase the finding accuracy. A two-tier process docking platform was selected that uses PatchDock and FireDock (Mashiach *et al*., 2008). The data generated included shape complementarity score and the best score was given by 2C helicase (5420) > capsid (5026) > 3D RNA polymerase (4918) > 2A protease (4904) > 3C protease (4792). 2C helicase and capsid (scores greater than 5000) stood out from the other target proteins by having

high geometric matches between protein and ligand structures, with interface areas of 688.50 and 673.00, respectively. Prodigiosin matched the protein's active pocket, thus having a high possibility of blocking the protein from functioning. However, the coarse global search algorithm by PatchDock evaluated only the compatibility of the ligand orientation to the active site by assuming proteins as one rigid body without permitting the protein conformational change calculation during interaction (Schneidman-Duhovny *et al*., 2005). Hence, to increase the data reading accuracy, further docking analysis was carried out with an interaction refinement process.

Proteins in real physiological conditions are dynamic and flexible. Therefore, the movements of the protein side chain and backbone have to be taken into account (May & Zacharias, 2005; Bonvin, 2006). Protein-ligand complexes with the best orientation scores for each target protein were further refined and re-scored to obtain the final global energy values. The results revealed that 2C helicase (-48.01 kcal/moL) > capsid (-36.52 kcal/moL) > 3C protease (-34.16 kcal/moL) > 3D RNA polymerase (-30.93 kcal/moL) > 2A protease (-20.61 kcal/moL) with the low-energy candidates (highly negative) ranked first. Using the same docking platform, Gupta *et al*. (2013) reported that the global energy of antiviral compounds ranges from -26.50 kcal/moL to -43.20 kcal/moL, to be potent drug candidates. Values in the same range were also discovered in this analysis, bolstering the initial findings that predicted prodigiosin has the potential to be developed as a potent antiviral drug based on the good energy values obtained after two consecutive dockings. The more negative the global energy of a complex, the more the complex binding free energy (thermodynamically favorable as the reaction is more stable and spontaneous) (Du *et al*., 2016). For this reason, 2C Helicase

was discovered to interact with the ligand more spontaneously and easily than the other target proteins.

Overall, *in silico* analysis found that three EV71 target proteins, namely 2C helicase, 3C protease, and capsid, exhibited the best interactions with prodigiosin. DockThor suggested 3C protease with the best binding affinity value (-8.162 kcal/moL) but gave the lowest value for PatchDock shape complementarity value (4792) and the third highest for FireDock global energy value (-34.16 kcal/moL). On the contrary, DockThor suggested 2C helicase with the third highest binding affinity value (-8.018 kcal/moL) but the highest values for both PatchDock shape complementarity value (5420) and FireDock global energy value (-48.01 kcal/moL). Interestingly, both PatchDock and FireDock suggested capsid as a consistent target protein alongside 2C helicase as the shape complementarity score and global energy value were not too far off between analyses. Hence, appropriate to the target protein functions, prodigiosin was predicted to be effective in the inhibition of early-phase transcription, polyprotein processing, and EV71 structural protein destruction. With this computational analysis evidence, it could be concluded that prodigiosin might be suitable to be used as a virucidal drug and a potent antivirus in post-treatment applications. In comparison to the prodigiosin *in silico* studies reported by Suba *et al*. (2013) against HBV, HIV, and H1N1, the results were comparable to that of this study. The protein-ligand binding affinities revealed were -8.87 kcal/moL for HBV, -8.14 kcal/moL for HIV, and -15.71 kcal/moL for H1N1, while it ranged from -6.113 kcal/moL to -8.162 kcal/moL for EV71 target proteins, with global energies ranging from -20.61 kcal/moL to -48.01 kcal/moL.

Protein-ligand complexes and interacting amino acid residues visualization

To ease the search for active sites which allow tight binding by prodigiosin, only those amino acid residues of the target proteins positioned within the 5 Å (atomic distance) range were considered for analysis using PyMOL. All of the amino acid residues in the 5 Å vicinity of prodigiosin were illustrated in a stick model, followed by the search for polar contacts with atoms. Dashed lines represent the bonds formed. Table 3 shows PyMOL visualization on bond formation in protein-ligand complexes, interacting amino acid residues' position in the protein chains as well as the interacting atoms' nucleus-to-nucleus distance.

Capsid interacted with prodigiosin, forming two hydrogen bonds with the Gln-30 and Asn-223 amino acid residues at a distance of 2.2 Å and 3.2 Å, respectively. The nucleus-to-nucleus distance given was within the range of a strong hydrogen bond (~2.5 Å to 3.5 Å). 2A protease, a cysteine protease with approximately 150 amino acids (Mu *et al*., 2013; Yuan *et al*., 2018), interacted with prodigiosin, forming one hydrogen bond directly to Trp-142 at a nucleus-to-nucleus distance of 4.6 Å. This weak hydrogen bond was taken into account after considering the possible movements of interacting molecular side chains and backbones. Apart from that, prodigiosin also formed a hydrogen bond with a nearby water molecule at a 4.5 Å distance and was potentially bonded to Trp-33 (4.9 Å). Due to the high likelihood of hydrogen bond formation with other surrounding water molecules in physiological conditions, these bonds were considered. In addition, these findings were constrained by the restricted presence of atoms within the protein crystal structures deposited in the PDB.

The 2C helicase, which is involved in genomic transcription and replication and is comprised of about 329 amino acids (Borowski *et al*., 2002; Yuan *et al*., 2018), was complexed with prodigiosin, forming as many as four hydrogen bonds between different amino acid residues within a strong hydrogen bond distance range of 2.5 Å until 3.4 Å. Prodigiosin bonded to Tyr-150, His-151, Gln-169, and Ser-212 at a nucleus-to-nucleus distance of 2.5 Å, 3.4 Å, 2.8 Å and 3.2 Å, respectively. The 3C protease, a cysteine protease made up of 184 amino acids (Cui *et al*., 2011; Yuan *et al*., 2018), interacted with prodigiosin as prodigiosin was shown to form a strong hydrogen bond with Glu-50 with a nucleus-to-nucleus distance of 2.7 Å. Lastly, 3D RNA polymerase, which consists of 462 amino acids (among the longest EV71 protein chain) complexed with prodigiosin as prodigiosin formed bonds with Ala-239 (3.6 Å) from the water molecule (2.4 Å) and to the aromatic ring of Tyr-237 (5.0 Å). Prodigiosin was found to have very weak interactions between water molecules and Ala-239. Also, the bond to the Tyr-237 aromatic ring made from one of the nitrogen atoms in the first pyrrole ring of prodigiosin results in hydrophobic contact with a weak interaction due to its formation at the maximum atomic nucleus-to-nucleus distance setting at a resolution of 5.0 Å.
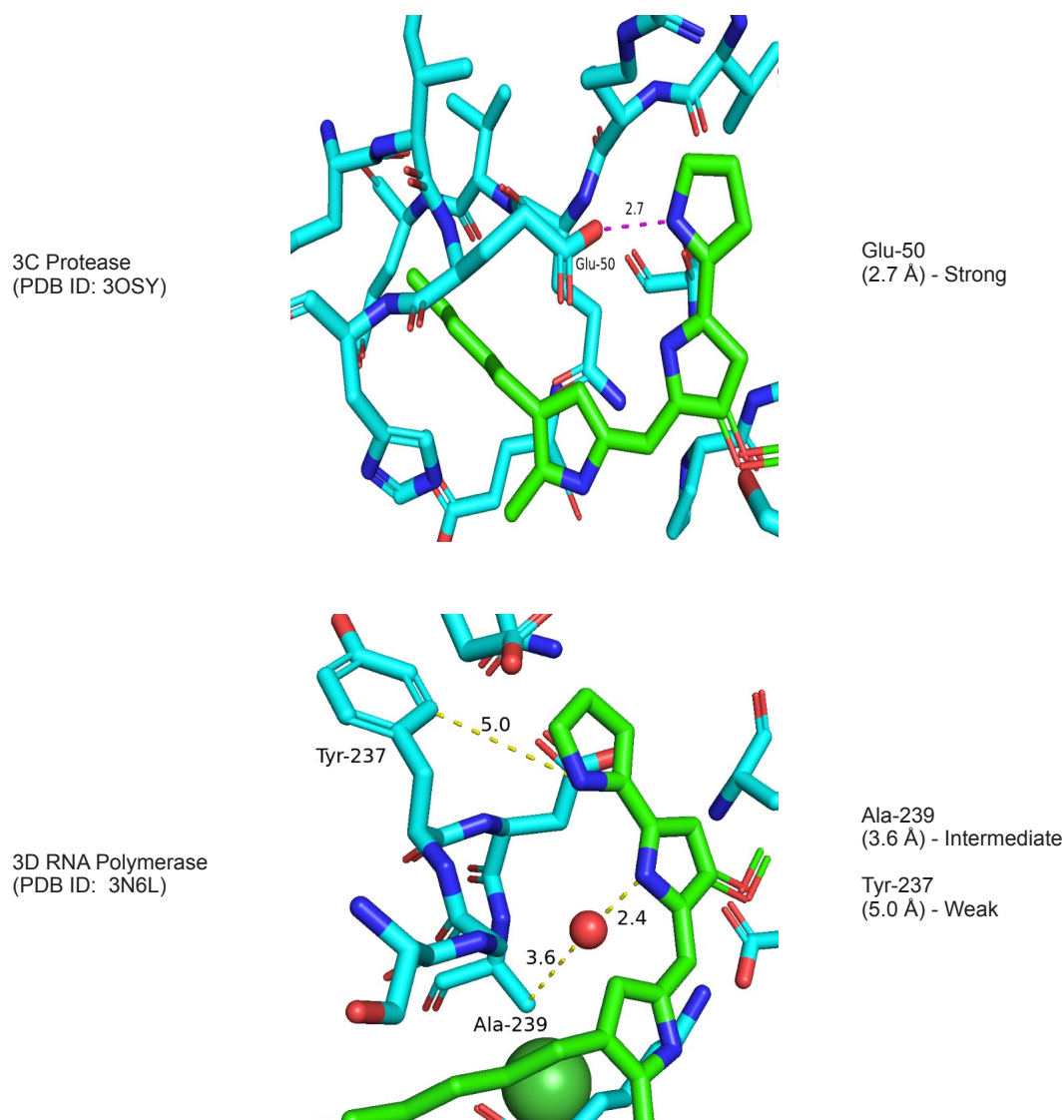
Results from prodigiosin interactions with the five target proteins of EV71 were compared and summarized in Table 4. According to the nucleus-to-nucleus distance of interacting atoms, it was concluded that prodigiosin could form strong bonds with 2C Helicase (all four strong bonds), Capsid (all two strong bonds), and 3C Protease (one strong bond). Meanwhile, only the intermediate bond with 3D RNA Polymerase and the weakest bond with 2A Protease (all two weak bonds). This result and position ranking between target proteins were by the global energy analysis from FireDock where 2C Helicase (-48.01 kcal/moL) > Capsid (-36.52

Table 3. Protein-ligand complexes and chemical bonds to amino acid residues

EV71 target protein	PyMOL visualization	Interacting amino acid, distance, and binding strength
Capsid (PDB ID: 3VBH)		Gln-30 (2.2 Å) - Strong Asn-223 (3.2 Å) - Strong
2A Protease (PDB ID: 3W95)		Trp-33 (4.9Å) - Weak Trp-142 (4.6 Å) - Weak
2C Helicase (PDB ID: 5GQ1)		Tyr-150 (2.5 Å) - Strong His-151 (3.4 Å) - Strong Gln-169 (2.8 Å) - Strong Ser-212 (3.2 Å) - Strong

Table 3 continued...

3C Protease
(PDB ID: 3OSY)

Glu-50
(2.7 Å) - Strong

3D RNA Polymerase
(PDB ID: 3N6L)

Ala-239
(3.6 Å) - Intermediate

Tyr-237
(5.0 Å) - Weak

kcal/moL) > 3C Protease (-34.16 kcal/moL) > 3D RNA Polymerase (-30.93 kcal/moL) > 2A Protease (-20.61 kcal/moL) and therefore could be made as a review of the results that reinforce previous initial findings.

Prodigiosin identification

Spectrophotometry analysis of the red pigment from *S. marcescens* UKMCC 1014 was revealed to have a maximal absorbance value at the 535 nm wavelength (λ). This value showed a resemblance to the absorbance spectrum characteristics of prodigiosin reported in previous studies with a maximal absorbance peak at λ=535 nm (De Araújo *et al.*, 2010; Elahian *et al.*, 2013; Lapenda *et al.*, 2014; Nakashima *et al.*, 2005; Song *et al.*, 2006).

In this study, red pigment from the methanolic extraction showed a maximal absorbance peak at λ=535 nm with an absorbance value (Abs) of 0.61 (Figure 1a). In the acidic solution, prodigiosin is red, showing a sharp, high, and narrow spectral band with a maximum at λ=535-540 nm and a slight shoulder on the low λ limb of the curve (about 510 nm) that is always present without any association with the impurity (Hubbard & Rimington, 1950). The same observation was also made in this study and this suggested that the pure red pigment extracted was the prodigiosin with sufficient quality and purity.

The methanol solvent (blank) displayed a maximal absorbance peak around λ=200 nm with an absorbance value (Abs) of 0.67, as

Table 4. Comparison of binding strength in the interaction of prodigiosin with amino acid residues

Target protein	Binding strength		
	Strong	Intermediate	Weak
Capsid	Gln-30 (2.2 Å)		
	Asn-223 (3.2 Å)		
2A Protease			Trp-33 (4.9 Å)
			Trp-142 (4.6 Å)
	Tyr-150 (2.5 Å)		
2C Helicase	His-151 (3.4 Å)		
	Gln-169 (2.8 Å)		
	Ser-212 (3.2 Å)		
3C Protease	Glu-50 (2.7 Å)		
3D RNA Polymerase		Ala-239 (3.6 Å)	Tyr-237 (5.0 Å)

well as a series of spectra spanning λ=200 nm to λ=300 nm (Figure 1b). The absorbance spectrum of the solvent explained the presence of the background absorbance noise in the low λ absorbance spectrum of the prodigiosin (Figure 1a). Organic solvents commonly have significant ultraviolet (UV) absorption and methanol showed weak absorbance at lower UV λ. The presence of methanol, the solvent used in pigment extraction, explained the presence of peaks other than the peak of prodigiosin. Additionally, there was a wide peak present at the wavelength of λ=350 nm and λ=400 nm in between the maximal absorbance peaks of the solvent and the prodigiosin in Figure 1a. This weak peak might have been due to the functional groups within the sample and it was required for further analysis using a Fourier transform infrared spectrophotometer (FTIR) for characterization.

Cytotoxicity assay

Cells were treated with prodigiosin at different concentrations (5-fold serial dilution) and the results were converted from absorbance value into cell viability percentage (%) as shown in Table 5. The results from the *in vitro* cell exposure to prodigiosin revealed that the pigment induced a cytotoxic effect at a high concentration and the effect was shown to be reduced gradually upon dilution of prodigiosin (dose-dependent) when compared to the control. The percentage of viable cells increased with the dose reduction of prodigiosin (inversely proportional). The value of cell viability percentage at each concentration of prodigiosin was calculated and the values were later presented as points on the Y-axis while the $\log_{10}$ concentrations of prodigiosin were presented as points on the X-axis in a graph (Figure 2).

Virucidal efficacy suspension test

The average virus titer (pfu/mL) was calculated from the observed number of plaques formed and the calculated titer reduction is tabulated in Table 6. Before treatment, the titer of the virus was found to be in the range of 1.0×10^6 pfu/mL to 3.0×10^6 pfu/mL.

The percentage of virus titer that had been successfully reduced after the mixture of the cell and the EV71 was exposed to prodigiosin was observed with time as a changing variable. For a 30-min time interval, the virus titer showed a reduction from 1.0×10^6 pfu/mL to 6.7×10^5 pfu/mL (and 3.3×10^5 pfu/mL difference after treatment). For a 60-min time interval, the virus titer showed a reduction from 2.0×10^6 pfu/mL to 1.3×10^6 pfu/mL (and 7.0×10^5 pfu/mL difference after treatment). This result revealed that there was a titer reduction occurring after treatment with prodigiosin with an intermediate inhibition effect via virucidal action. The two contact times were chosen by the standard procedure in evaluating virucidal efficacy suspension tests, which range from 30 sec to no more than 60 min (Rabenau *et al*., 2020). Any activities demonstrated after the time limit may render the active compound ineffective in the intended area of usage due to unrealistic contact time. Additionally, the reduction resulting from prolonged contact times may be invalid as the number of viral particles will gradually decrease when they are outside of host cells for an extended period, even in the absence of treatment.

To date, there are numerous reports regarding natural compounds that have a virucidal effect against EV71. Li *et al*. (2020) reported the acidic polysaccharide extract from *Laminaria japonica* as having good virucidal activity against EV71 by direct inactivation of the virus, preventing
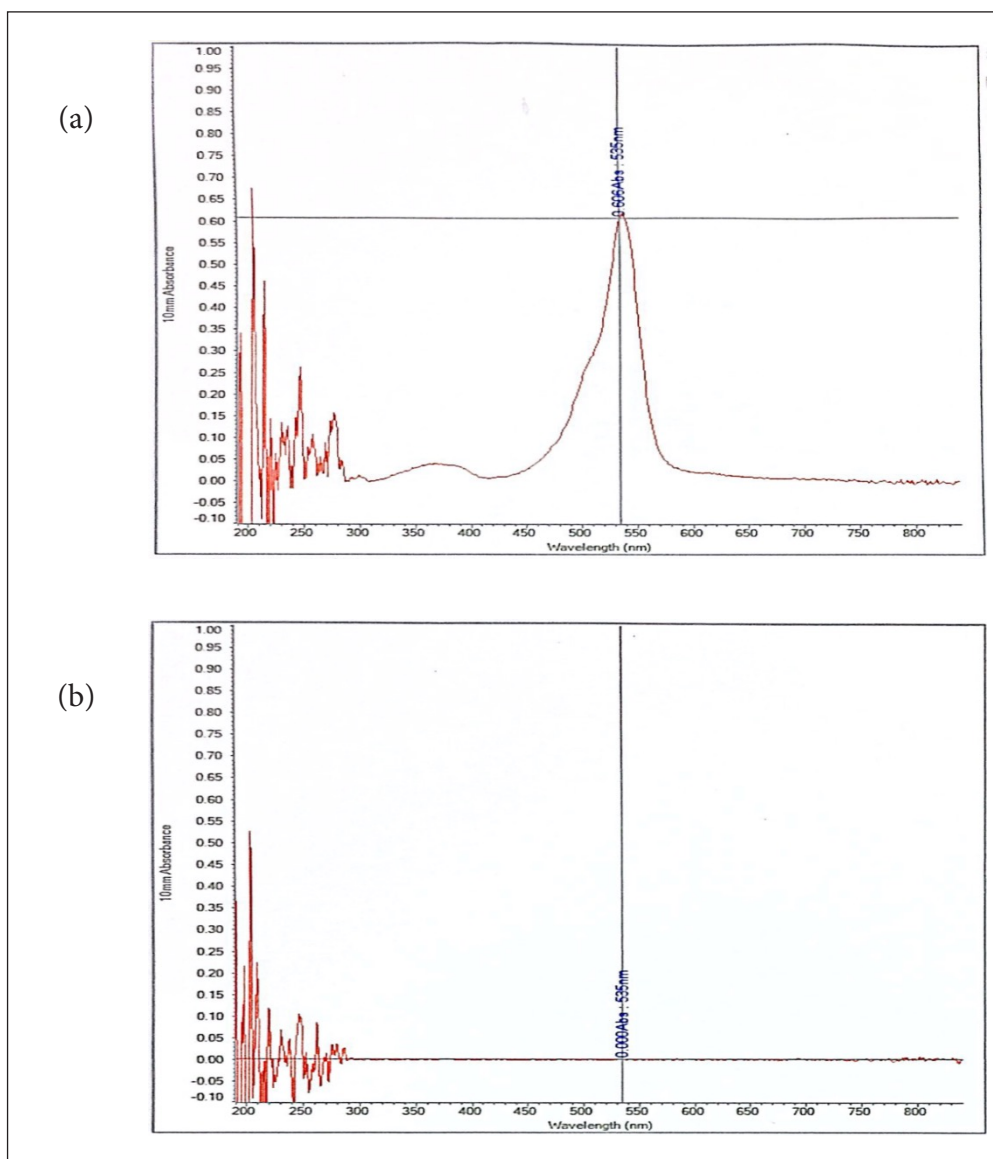
Fig. 1. The absorbance spectrum for the (a) red pigment (prodigiosin) and (b) solvent.

Table 5. Cell viability percentage average after the prodigiosin treatment

[Prodigiosin], μg/mL	Absorbance Reading Average at 570 nm for Prodigiosin-treated Cell, Abs	Cell Viability Percentage Average for Prodigiosin-treated Cell, %
40	0.1440 ± 0.00	1.74 ± 0.21
8	0.1995 ± 0.01	5.74 ± 0.56
1.6	1.0200 ± 0.03	64.94 ± 2.04
0.32	0.9075 ± 0.02	56.82 ± 1.58
0.064	1.3275 ± 0.03	87.12 ± 1.99
0.0128	1.7695 ± 0.10	119.01 ± 6.89
0.00256	1.7440 ± 0.05	117.17 ± 3.87
0.000512	1.7020 ± 0.01	114.14 ± 0.61
0.0001024	1.7160 ± 0.13	115.15 ± 9.39
0.00002048	1.5025 ± 0.01	99.75 ± 0.76

Control	Absorbance Reading Average at 570 nm for Control, Abs
Positive	1.5063 ± 0.06
Negative	0.1203 ± 0.01

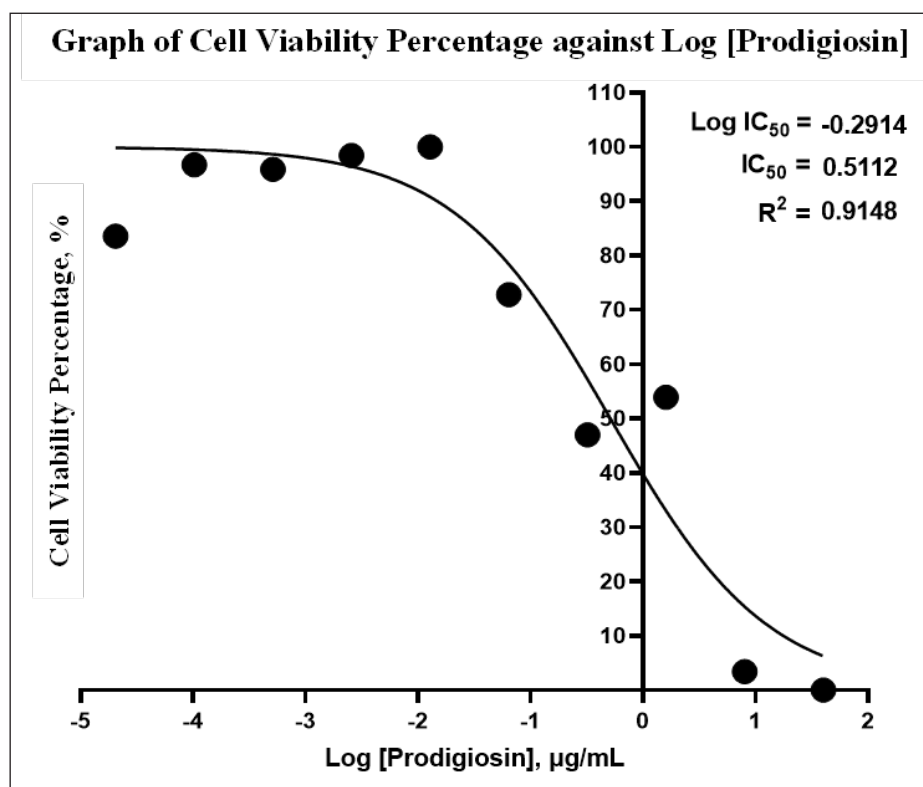*T-test provided $p<0.05$ at 40, 8, 1.6, and 0.32 μg/mL [Prodigiosin] when compared to control

Fig. 2. Graph of cell viability percentage, % against Log_{10} [prodigiosin], μg/mL. The graph was used to calculate the IC_{50} value after treatment.

Table 6. Virus titer reduction with 10^{-5} dilution at 30- and 60-min time intervals

	Virus titer average (pfu/mL)	
	30-min	60-min
Prodigiosin-treated*	$6.7 \times 10^5 \pm 5.8 \times 10^5$	$1.3 \times 10^6 \pm 5.8 \times 10^5$
Negative control#	$1.0 \times 10^6 \pm 0.0$	$2.0 \times 10^6 \pm 1.4 \times 10^6$
Log_{10} titer reduction	0.17	0.19
Titer reduction percentage	32.39%	35.43%

*n=3 (prodigiosin-treated)
#n=2 (negative control) for each time interval

attachments but demonstrating weak inhibition for post-treatment. Apart from that, natural products reported with anti-EV71 activity include allophycocyanin (Shih *et al*., 2003), raoulic acid (Choi *et al*., 2009), chrysosplenetin and penduletin (Zhu *et al*., 2011), and matrine (Yang *et al*., 2012). The abovementioned natural compounds, including prodigiosin, have shown virucidal activity against EV71 by targeting crucial viral proteins in multiple stages of viral replication, which have been identified as primary drug targets. Consistent with our findings, most of these compounds were suggested to interfere with the early stages of the viral replication cycle (in adsorption, penetration, and RNA replication), except matrine, which was shown to regulate host immune response (*in vivo*). Since highly efficacious natural compounds are extremely difficult to discover, structural modification and derivative synthesis may be considered to enhance their efficacy (Lin *et al*., 2022; Xu *et al*., 2022). Furthermore, Shang, Xu, and Yin (2013) reported that 6-amino acid peptide (LVLQTM) was capable of binding the active site and inhibiting 2A protease (Falah *et al*., 2012), metrifudil and N6-benzyladenosine inhibited 2C helicase (Arita *et al*., 2008), and rupintrivir inhibited 3C protease (Kuo *et al*., 2008; Cui *et al*., 2011; Tan *et al*., 2016). Unfortunately, no clinical trials have been reported to have been successfully initiated. The discovery of antiviral activity with prophylactic and preemptive characteristics in natural compounds is significantly low as compared to post-treatment targets (therapeutic) and in synthetic compounds. Therefore, a continuous effort to search for compounds having antiviral activity against EV71 is crucial to discovering compounds that could pass a clinical trial.

Log_{10} reduction of titer given 0.17 and 0.19 by prodigiosin at 30-min and 60-min time intervals. The percentage of titer reduction calculated at 0.17 log reduction and 0.19 log reduction was 32.39% and 35.43% for a 30-min and 60-min time interval, respectively. The given values were considered low since the titer reduction of at least 4 log_{10}, which is equivalent to a reduction percentage of 99.99%, permits the product tested to be concluded to have virus-inactivating properties (strong inhibition effect) under specified test conditions (Rabenau *et al*., 2020). In this study, prodigiosin demonstrated a weak ability to inactivate EV71 and virucidal activity with an intermediate inhibition effect. Moreover, it was also found that the result of the percentage of titer reduction did not show a doubling in titer reduction, even though the contact time had doubled. Still, prodigiosin showed a slightly higher reduction of virus titer at the longer 60-min treatment time (contact time) as compared to the shorter 30-min contact time. However, the differences in the titer reduction between those

time intervals were not as significant, resulting in the 30-min treatment time being seen as more effective. This data suggested that prodigiosin was capable of inactivating EV71 (intermediate inhibition) while demonstrating efficacy *in vitro*, under test conditions (dilution and contact time-point).

Also, the intermediate inhibition effect might be due to the low concentration of prodigiosin used which was insufficient to inhibit the non-enveloped EV71, which is a highly resistant virus. Hayashi *et al*. (2019) reported that the application of a higher concentration than CC_{50} increased the effectiveness of a compound *in vivo* testing compared to *in vitro* testing. Therefore, if prodigiosin is to be developed as a topical drug for HFMD, a higher concentration that is more cytotoxic could be used for external usage. Additionally, there are many different strategies thought to apply to increasing chemical compound effectiveness, including the combination of several antiviral drugs to give a synergistic effect that is more effective, as reported by Criscuolo *et al*. (2018), Lin *et al*. (2016) and Zhang *et al*. (2014). The synergistic action was reported to be able to overcome the side effects produced as a result of high dosages of single-target drugs, increased the selectivity of the drug, and could provide highly accurate biological systems control (Lehár *et al*., 2009).

All in all, prodigiosin has been proven to possess *in vitro* virucidal activity to inactivate EV71. This observation confirmed the preliminary findings from the *in silico* analysis which suggested the ability of prodigiosin to strongly interact with the viral capsid protein, suggesting potential virucidal action. The unequal variance two-tailed paired t-test showed that the activity difference at 30-min and 60-min time intervals did not have a significant difference after treatment due to the *p*-value (probability) of .4226 and .6244, respectively. The inhibition of the capsid protein prevented receptor binding by the virus in the early phase of its life cycle. As for other proteins targeting different stages of the EV71 life cycle that provided convincing results through molecular docking still requires further post-treatment studies for confirmation.

CONCLUSION

In silico studies have suggested that prodigiosin is a potent antiviral drug candidate against EV71. The 2C helicase (-48.01 kcal/moL) had the most negative global energy value, followed by the capsid (-36.52 kcal/moL), 3C protease (-34.16 kcal/moL), 3D RNA polymerase (- 30.93 kcal/moL), and 2A protease (-20.61 kcal/moL) in the interaction refinement analysis using FireDock. Prodigiosin, in the interactions, formed bonds with the amino acid residues on the capsid (Gln-

30, Asn-223), 2A protease (Trp-33, Trp-142), 2C helicase (Tyr-150, His-151, Gln-169, Ser-212), 3C protease (Glu-50) and 3D RNA polymerase (Ala-239, Tyr-237). *In vitro* studies have successfully identified prodigiosin as the red pigment extracted from *S. marcescens* UKMCC 1014 using methanolic extraction, with an IC_{50} value of 0.5112 µg/mL of prodigiosin concentration. Furthermore, the virucidal efficacy suspension test revealed that prodigiosin (1.6 µg/mL) at 10^{-5} dilution had a 0.17 log reduction (32.39%) and a 0.19 log reduction (35.43%) of virus titer at a 30-min and 60-min time interval, respectively. In this study, prodigiosin was found to have intermediate virucidal antiviral activity. Hence, this latest discovery of the antiviral property of prodigiosin against EV71 adds to the already extensive list of its reported biological activities.

ACKNOWLEDGEMENTS

CONFLICT OF INTEREST
The authors declare no conflict of interest.

REFERENCES

Abdullah, N.H. 2022. Situasi semasa kejadian penyakit tangan, kaki dan mulut (HFMD) di Malaysia [WWW Document]. URL https://kpkesihatan.com/2022/06/14/kenyataan-akhbar-kpk-14-jun-2022-situasi-semasa-kejadian-penyakit-tangan-kaki-dan-mulut-hfmd-di-malaysia-me-23-2022/ (accessed 9.11.2022).

Andrusier, N., Nussinov, R. & Wolfson, H.J. 2007. FireDock: Fast interaction refinement in molecular docking. Proteins: Structure, Function and Genetics, 69(1): 139–159. https://doi.org/10.1002/prot.21495

Arita, M., Wakita, T. & Shimizu, H. 2008. Characterization of pharmacologically active compounds that inhibit poliovirus and enterovirus 71 infectivity. Journal of General Virology, 89(10): 2518–2530. https://doi.org/10.1099/vir.0.2008/002915-0

Bonvin, A.M. 2006. Flexible protein-protein docking. Current Opinion in Structural Biology, 16(2): 194–200. https://doi.org/10.1016/j.sbi.2006.02.002

Borowski, P., Niebuhr, A., Schmitz, H., Hosmane, R.S., Bretner, M., Siwecka, M.A. & Kulikowski, T. 2002. NTPase/helicase of Flaviviridae: inhibitors and inhibition of the enzyme. Acta Biochimica Polonica, 49(3): 597–614.

Cai, Q., Yameen, M., Liu, W., Gao, Z., Li, Y., Peng, X., Cai, Y., Wu, C., Zheng, Q., Li, J. & Lin, T. 2013. Conformational plasticity of the 2A proteinase from Enterovirus 71. Journal of Virology, 87(13): 7348–7356. https://doi.org/10.1128/jvi.03541-12

CDC. 2022. Hand, foot, and mouth disease [WWW Document]. URL https://wwwnc.cdc.gov/travel/diseases/hand-foot-and-mouth-disease (accessed 9.11.2022).

Chen, C., Wang, Y., Shan, C., Sun, Y., Xu, P., Zhou, H., Yang, C., Shi, P.Y., Rao, Z., Zhang, B. & Lou, Z. 2013. Crystal structure of Enterovirus 71 RNA-dependent RNA polymerase complexed with its protein primer VPg: implication for a trans mechanism of VPg uridylylation. Journal of Virology, 87(10): 5755–5768. https://doi.org/10.1128/jvi.02733-12

Choi, H.J., Lim, C.H., Song, J.H., Baek, S.H. & Kwon, D.H. 2009. Antiviral activity of raoulic acid from *Raoulia australis* against Picornaviruses. Phytomedicine, 16(1): 35–39. https://doi.org/10.1016/j.phymed.2008.10.012

Chua, K.B. & Kasri, A.R. 2011. Hand foot and mouth disease due to Enterovirus 71 in Malaysia. Virologica Sinica, 26(4): 221–228. https://doi.org/10.1007/s12250-011-3195-8

Coates, S.J., Davis, M.D.P. & Andersen, L.K. 2019. Temperature and humidity affect the incidence of hand, foot, and mouth disease: A systematic review of the literature - a report from the International Society of Dermatology Climate Change Committee. International Journal of Dermatology, 58(4): 388–399. https://doi.org/10.1111/ijd.14188

Criscuolo, E., Clementi, N., Mancini, N., Burioni, R., Miduri, M., Castelli, M. & Clementi, M. 2018. Synergy evaluation of anti-Herpes Simplex Virus type 1 and 2 compounds acting on different steps of virus life cycle. Antiviral Research, 151(3): 71–77. https://doi.org/10.1016/j.antiviral.2018.01.009

Cui, S., Wang, J., Fan, T., Qin, B., Guo, L., Lei, X., Wang, J., Wang, M. & Jin, Q. 2011. Crystal structure of human enterovirus 71 3C protease. Journal of Molecular Biology, 408(3): 449–461. https://doi.org/10.1016/j.jmb.2011.03.007

De Araújo, H.W.C., Fukushima, K. & Takaki, G.M.C. 2010. Prodigiosin production by *Serratia marcescens* UCP 1549 using renewable-resources as a low cost substrate. Molecules, 15(10): 6931–6940. https://doi.org/10.3390/molecules15106931

Du, X., Li, Y., Xia, Y.L., Ai, S. M., Liang, J., Sang, P., Ji, X.L. & Liu, S.Q. 2016. Insights into protein–ligand interactions: mechanisms, models, and methods. International Journal of Molecular Sciences, 17(2):

144. https://doi.org/10.3390/ijms17020144

Elahian, F., Moghimi, B., Dinmohammadi, F., Ghamghami, M., Hamidi, M. & Mirzaei, S.A. 2013. The anticancer agent prodigiosin is not a multidrug resistance protein substrate. DNA and Cell Biology, 32(3): 90–97. https://doi.org/10.1089/dna.2012.1902

Falah, N., Montserret, R., Lelogeais, V., Schuffenecker, I., Lina, B., Cortay, J.C. & Violot, S. 2012. Blocking human enterovirus 71 replication by targeting viral 2A protease. Journal of Antimicrobial Chemotherapy, 67(12): 2865–2869. https://doi.org/10.1093/jac/dks304

Fang, C.Y. & Liu, C.C. 2018. Recent development of Enterovirus A vaccine candidates for the prevention of hand, foot, and mouth disease. Expert Review of Vaccines, 17(9): 819–831. https://doi.org/10.1080/14760584.2018.1510326

Fong, S.Y., Mori, D., Rundi, C., Yap, J.F., Jikal, M., Latip, A.L.L.B.A., Johnny, V. & Ahmed, K. 2021. A five-year retrospective study on the epidemiology of hand, foot and mouth disease in Sabah, Malaysia. Scientific Reports, 11(1): 17814. https://doi.org/10.1038/S41598-021-96083-3

Guan, H., Tian, J., Qin, B., Wojdyla, J.A., Wang, B., Zhao, Z., Wang, M. & Cui, S. 2017. Crystal structure of 2C helicase from enterovirus 71. Science Advances, 3(4): e1602573. https://doi.org/10.1126/sciadv.1602573

Gupta, S.K., Singh, S., Nischal, A., Pant, K.K. & Seth, P.K. 2013. Molecular docking and simulation studies towards exploring antiviral compounds against envelope protein of Japanese encephalitis virus. Network Modeling and Analysis in Health Informatics and Bioinformatics, 2(4): 231–243. https://doi.org/10.1007/s13721-013-0040-z

Hayashi, K., Lee, J. B., Atsumi, K., Kanazashi, M., Shibayama, T., Okamoto, K., Kawahara, T. & Hayashi, T. 2019. In vitro and in vivo anti-herpes simplex virus activity of monogalactosyl diacylglyceride from *Coccomyxa* sp. KJ (IPOD FERM BP-22254), a green microalga. PLoS ONE, 14(7): e0219305. https://doi.org/10.1371/journal.pone.0219305

Hubbard, R. & Rimington, C. 1950. The biosynthesis of prodigiosin, the tripyrrylmethene pigment from *Bacillus prodigiosus* (*Serratia marcescens*). Biochemical Journal, 46(2): 220–225. https://doi.org/10.1042/bj0460220

Kim, B., Moon, S., Bae, G.R., Lee, H., Pai, H. & Oh, S.H. 2018. Factors associated with severe neurologic complications in patients with either hand-foot-mouth disease or herpangina: A nationwide observational study in South Korea, 2009-2014. PLOS ONE, 13(8): e0201726. https://doi.org/10.1371/journal.pone.0201726

Kuo, C.J., Shie, J.J., Fang, J.M., Yen, G.R., Hsu, J.T.A., Liu, H.G., Tseng, S.N., Chang, S.C., Lee, C.Y., Shih, S.R. & Liang, P.H. 2008. Design, synthesis, and evaluation of 3C protease inhibitors as anti-enterovirus 71 agents. Bioorganic and Medicinal Chemistry, 16(15): 7388–7398. https://doi.org/10.1016/j.bmc.2008.06.015

Lapenda, J.C., Silva, P.A., Vicalvi, M.C., Sena, K.X.F.R. & Nascimento, S.C. 2015. Antimicrobial activity of prodigiosin isolated from *Serratia marcescens* UFPEDA 398. World Journal of Microbiology and Biotechnology, 31(2): 399–406. https://doi.org/10.1007/s11274-014-1793-y

Lapenda, L.J., Maciel, C., Xavier, H., Alves, da S.C. & Takaki, G.M.C. 2014. Production and toxicological evaluation of prodigiosin from *Serratia marcescens* UCP/WFCC1549 on mannitol solid medium. International Journal of Applied Research in Natural Products, 7(2): 32–38.

Lehár, J., Krueger, A.S., Avery, W., Heilbut, A.M., Johansen, L.M., Price, E.R., Rickles, R.J., Short Iii, G.F., Staunton, J.E., Jin, X. & Lee, M.S. 2009. Synergistic drug combinations tend to improve therapeutically relevant selectivity. Nature Biotechnology, 27(7): 659–666. https://doi.org/10.1038/nbt.1549

Lei, X., Cui, S., Zhao, Z. & Wang, J. 2015. Etiology, pathogenesis, antivirals and vaccines of hand, foot, and mouth disease. National Science Review, 2(3): 268–284. https://doi.org/10.1093/nsr/nwv038

Li, M.L., Lin, J.Y., Chen, B.S., Weng, K.F., Shih, S.R., Calderon, J.D., Tolbert, B.S. & Brewer, G. 2019. EV71 3C protease induces apoptosis by cleavage of hnRNP A1 to promote apaf-1 translation. PLOS ONE, 14(9): e0221048. https://doi.org/10.1371/journal.pone.0221048

Li, M. L., Shih, S. R., Tolbert, B. S. & Brewer, G. 2021. Enterovirus a71 vaccines. Vaccines, 9(3): 1–10. https://doi.org/10.3390/VACCINES9030199

Li, Y., Yu, J., Qi, X. & Yan, H. 2019. Monoclonal antibody against EV71 3D^{pol} inhibits the polymerase activity of RdRp and virus replication. BMC Immunology, 20(1): 6. https://doi.org/10.1186/s12865-019-0288-x

Li, Z., Cui, B., Liu, X., Wang, L., Xian, Q., Lu, Z., Liu, S., Cao, Y. & Zhao, Y. 2020. Virucidal activity and the antiviral mechanism of acidic polysaccharides against Enterovirus 71 infection in vitro. Microbiology and Immunology, 64(3): 189–201. https://doi.org/10.1111/1348-0421.12763

Lin, B., He, S., Yim, H.J., Liang, T.J. & Hu, Z. 2016. Evaluation of antiviral drug synergy in an infectious

HCV system. Antiviral Therapy, 21(7): 595–603. https://doi.org/10.3851/IMP3044

Lin, C., Jia, X., Fang, Y., Chen, L., Zhang, H., Lin, R. & Chen, J. 2019. Enhanced production of prodigiosin by *Serratia marcescens* FZSF02 in the form of pigment pellets. Electronic Journal of Biotechnology, 40: 58–64. https://doi.org/10.1016/j.ejbt.2019.04.007

Lin, D., Jiang, S., Zhang, A., Wu, T., Qian, Y. & Shao, Q. 2022. Structural derivatization strategies of natural phenols by semi-synthesis and total-synthesis. Natural Products and Bioprospecting, 12(1): 1–29. https://doi.org/10.1007/S13659-022-00331-6

Lin, J.Y., Kung, Y.A. & Shih, S.R. 2019. Antivirals and vaccines for Enterovirus A71. *J*ournal of Biomedical Science, 26(1): 1–10. https://doi.org/10.1186/s12929-019-0560-7

Littler, D.R., Liu, M., McAuley, J.L., Lowery, S.A., Illing, P.T., Gully, B.S., Purcell, A.W., Chandrashekaran, I.R., Perlman, S., Purcell, D.F. & Quinn, R.J. 2021. A natural product compound inhibits coronaviral replication in vitro by binding to the conserved Nsp9 SARS-CoV-2 protein. Journal of Biological Chemistry, 297(6): 101362. https://doi.org/10.1016/J.JBC.2021.101362

Mashiach, E., Schneidman-Duhovny, D., Andrusier, N., Nussinov, R. & Wolfson, H.J. 2008. FireDock: a web server for fast interaction refinement in molecular docking. Nucleic acids research, 36(Web Server issue): 229–232. https://doi.org/10.1093/nar/gkn186

May, A. & Zacharias, M. 2005. Accounting for global protein deformability during protein-protein and protein-ligand docking. Biochimica et Biophysica Acta - Proteins and Proteomics, 1754(1–2): 225–231. https://doi.org/10.1016/j.bbapap.2005.07.045

Mu, Z., Wang, B., Zhang, X., Gao, X., Qin, B., Zhao, Z. & Cui, S. 2013. Crystal structure of 2A proteinase from hand, foot and mouth disease virus. Journal of Molecular Biology, 425(22): 4530–4543. https://doi.org/10.1016/j.jmb.2013.08.016

Nakashima, T., Kurachi, M., Kato, Y., Yamaguchi, K. & Oda, T. 2005. Characterization of bacterium isolated from the sediment at coastal area of Omura Bay in Japan and several biological activities of pigment produced by this isolate. Microbiology and Immunology, 49(5): 407–415. https://doi.org/10.1111/j.1348-0421.2005.tb03744.x

Peele, K.A., Potla Durthi, C., Srihansa, T., Krupanidhi, S., Ayyagari, V.S., Babu, D.J., Indira, M., Reddy, A.R. & Venkateswarulu, T.C. 2020. Molecular docking and dynamic simulations for antiviral compounds against SARS-CoV-2: A computational study. Informatics in Medicine Unlocked, 19: 100345. https://doi.org/10.1016/j.imu.2020.100345

Pourianfar, H.R. & Grollo, L. 2015. Development of antiviral agents toward enterovirus 71 infection. Journal of Microbiology, Immunology and Infection, 48(1): 1–8. https://doi.org/10.1016/j.jmii.2013.11.011

Protein Data Bank. 2022. Guide to Understanding PDB Data. URL https://pdb101.rcsb.org/learn/guide-to-understanding-pdb-data/resolution (accessed 12.23.2022).

Rabenau, H.F., Schwebke, I., Blümel, J., Eggers, M., Glebe, D., Rapp, I., Sauerbrei, A., Steinmann, E., Steinmann, J., Willkommen, H. & Wutzler, P . 2020. Guideline for testing chemical disinfectants regarding their virucidal activity within the field of human medicine. Bundesgesundheitsblatt, 63(5): 645–655. https://doi.org/10.1007/s00103-020-03115-w

Rasti, M., Khanbabaei, H. & Teimoori, A. 2019. An update on Enterovirus 71 infection and interferon type I response. Reviews in Medical Virology, 29(1): 2016. https://doi.org/10.1002/rmv.2016

Ren, J., Wang, X., Zhu, L., Hu, Z., Gao, Q., Yang, P., Li, X., Wang, J., Shen, X., Fry, E.E. & Rao, Z. 2015. Structures of Coxsackievirus A16 capsids with native antigenicity: Implications for particle expansion, receptor binding, and immunogenicity. Journal of Virology, 89(20): 10500–10511. https://doi.org/10.1128/JVI.01102-15

Schneidman-Duhovny, D., Inbar, Y., Nussinov, R. & Wolfson, H.J. 2005. PatchDock and SymmDock: servers for rigid and symmetric docking. Nucleic Acids Research, 33(2): 363–367. https://doi.org/10.1093/nar/gki481

Shang, L., Xu, M. & Yin, Z. 2013. Antiviral drug discovery for the treatment of enterovirus 71 infections. Antiviral Research, 97(2): 183–194. https://doi.org/10.1016/j.antiviral.2012.12.005

Shih, S.R., Tsai, K.N., Li, Y.S., Chueh, C.C. & Chan, E.C. 2003. Inhibition of enterovirus 71-induced apoptosis by allophycocyanin isolated from a blue-green alga *Spirulina platensis*. Journal of Medical Virology, 70(1): 119–125. https://doi.org/10.1002/jmv.10363

Song, M.J., Bae, J., Lee, D.S., Kim, C.H., Kim, J.S., Kim, S.W. & Hong, S.I. 2006. Purification and characterization of prodigiosin produced by integrated bioreactor from *Serratia* sp. KH-95. Journal of Bioscience and Bioengineering, 101(2): 157–161. https://doi.org/10.1263/jbb.101.157

Su, X., Wang, Q., Wen, Y., Jiang, S. & Lu, L. 2020. Protein- and peptide-based virus inactivators: Inactivating viruses before their entry into cells. Frontiers in Microbiology, 11: 1063. https://doi.org/10.3389/FMICB.2020.01063/BIBTEX

Suba, K., Stalin, A., Girija, A. & Raguraman, R. 2013. Homology modeling and docking analysis of prodigiosin from *Serratia marcescens*. Elixir International Journal, 55: 12897–12902.

Sun, B.J., Chen, H.J., Chen, Y., An, X.D. & Zhou, B.S. 2018. The risk factors of acquiring severe hand, Foot, and mouth disease: A meta-analysis. Canadian Journal of Infectious Diseases and Medical Microbiology, 2018 (eCollection): 1–12. https://doi.org/10.1155/2018/2751457

Tan, C.W., Poh, C.L., Sam, I.-C. & Chan, Y.F. 2013. Enterovirus 71 uses cell surface heparan sulfate glycosaminoglycan as an attachment receptor. Journal of Virology, 87(1): 611–620. https://doi.org/10.1128/jvi.02226-12

Tan, Y.W., Ang, M.J.Y., Lau, Q.Y., Poulsen, A., Ng, F.M., Then, S.W., Peng, J., Hill, J., Hong, W.J., Chia, C.S.B. & Chu, J.J.H. 2016. Antiviral activities of peptide-based covalent inhibitors of the Enterovirus 71 3C protease. Scientific Reports, 6(9): 1–9. https://doi.org/10.1038/srep33663

van der Linden, L., Wolthers, K.C. & van Kuppeveld, F.J.M. 2015. Replication and inhibitors of enteroviruses and parechoviruses. Viruses, 7(8): 4529–4562. https://doi.org/10.3390/v7082832

Wang, T., Wang, B., Huang, H., Zhang, C., Zhu, Y., Pei, B., Cheng, C., Sun, L., Wang, J., Jin, Q. & Zhao, Z. 2017. Enterovirus 71 protease 2Apro and 3Cpro differentially inhibit the cellular endoplasmic reticulum-associated degradation (ERAD) pathway via distinct mechanisms, and enterovirus 71 hijacks ERAD component p97 to promote its replication. PLoS Pathogens, 13(10): e1006674. https://doi.org/10.1371/journal.ppat.1006674

Wei, Y.H. & Chen, W.C. 2005. Enhanced production of prodigiosin-like pigment from *Serratia marcescens* SMAR by medium improvement and oil-supplementation strategies. Journal of Bioscience and Bioengineering, 99(6): 616–622. https://doi.org/10.1263/jbb.99.616

Wen, W., Qi, Z. & Wang, J. 2020. The function and mechanism of Enterovirus 71 (EV71) 3C protease. Current Microbiology, 77(9): 1968–1975. https://doi.org/10.1007/s00284-020-02082-4

Wlodawer, A., Minor, W., Dauter, Z. & Jaskolski, M. 2008. Protein crystallography for non-crystallographers, or how to get the best (but not more) from published macromolecular structures. FEBS Journal, 275(1): 1–21. https://doi.org/10.1111/j.1742-4658.2007.06178.x

World Health Organization. 2018. Hand, foot and mouth disease situation update 2018 [WWW Document]. URL https://apps.who.int/iris/handle/10665/274107 (accessed 9.12.2022).

Xia, H., Wang, P., Wang, G.C., Yang, J., Sun, X., Wu, W., Qiu, Y., Shu, T., Zhao, X., Yin, L. & Qin, C.F. 2015. Human enterovirus nonstructural protein 2CATPase functions as both an RNA helicase and ATP-independent RNA chaperone. PLOS Pathogens, 11(7): e1005067. https://doi.org/10.1371/journal.ppat.1005067

Xu, W.F., Wu, N.N., Wu, Y.W., Qi, Y.X., Wei, M.Y., Pineda, L.M., Ng, M.G., Spadafora, C., Zheng, J.Y., Lu, L. & Wang, C.Y. 2022. Structure modification, antialgal, antiplasmodial, and toxic evaluations of a series of new marine-derived 14-membered resorcylic acid lactone derivatives. Marine Life Science and Technology, 4(1): 88–97. https://doi.org/10.1007/S42995-021-00103-0

Yang, Y., Xiu, J., Zhang, X., Zhang, L., Yan, K., Qin, C. & Liu, J. 2012. Antiviral effect of matrine against human enterovirus 71. Molecules, 17(9): 10370–10376. https://doi.org/10.3390/molecules170910370

Yuan, J., Shen, L., Wu, J., Zou, X., Gu, J., Chen, J. & Mao, L. 2018. Enterovirus A71 proteins: Structure and function. Frontiers in Microbiology, 9(286): 1–8. https://doi.org/10.3389/fmicb.2018.00286

Yuan, S., Li, G., Wang, Y., Gao, Q., Wang, Y., Cui, R., Altmeyer, R. & Zou, G. 2016. Identification of positively charged residues in Enterovirus 71 capsid protein VP1 essential for production of infectious particles. Journal of Virology, 90(2): 741–752. https://doi.org/10.1128/jvi.02482-15

Zhang, C., Zhai, S., Li, X., Zhang, Q., Wu, L., Liu, Y., Jiang, C., Zhou, H., Li, F., Zhang, S. & Su, G. 2014. Synergistic action by multi-targeting compounds produces a potent compound combination for human NSCLC both in vitro and in vivo. Cell Death and Disease, 5(3): e1138–e1138. https://doi.org/10.1038/cddis.2014.76

Zhu, Q.C., Wang, Y., Liu, Y.P., Zhang, R.Q., Li, X., Su, W.H., Long, F., Luo, X.D. & Peng, T. 2011. Inhibition of enterovirus 71 replication by chrysosplenetin and penduletin. *European* Journal of Pharmaceutical Sciences, 44(3): 392–398. https://doi.org/10.1016/j.ejps.2011.08.030